Vol. 87 No. 6 pp. 1630–1642 ACTA GEOLOGICA SINICA (English Edition) Dec. 2013

# Metallogenic Model of Bauxite in Central Guizhou Province: an Example of Lindai Deposit

LING Kunyue[1, 2], ZHU Xiaoqing[1, *], WANG Zhonggang[1], HAN Tao[1], TANG Haoshu[1] and CHEN Wenyi[3]

1 *Institute of Geochemistry, Chinese Academy of Sciences, Guiyang 550002, Guizhou, China*
2 *University of Chinese Academy of Sciences, Beijing 100049, China*
3 *Institute of Geology, Guizhou Bureau of Geology and Minerals, Guiyang 550004, Guizhou, China*

**Abstract: The bauxites in central Guizhou are hosted by the Lower Carboniferous Jiujialu Formation. Geochemistrial characteristics of the Lindai bauxite deposit indicate that the underlying Shilengshui Formation dolomite is the precursor rock of mineral resources. Weathering simulation experiments show that Si is most likely to migrate with groundwater, the migration rate of which is several magnitude higher than Al and Fe under nature conditions (pH=3–9). The neutral and acid non-reducing condition is the most conducive to the Al rich and Si removal, while the acid reducing conditions is the most conducive to the Al rich and Fe removal. In the process of bauxite formation, coal beds overlying the Al-bearing rock series or other rock formation rich in organic materials can produce acid reducing groundwater, which are important for the bauxite formation. Finally, propose the metallogenic model of the bauxite in central Guizhou Province and put forward three new words which are "original bauxite material", "bauxite material" and "original bauxite".**

**Key words: bauxite, groundwater, geochemistrial characteristics, weathering simulation experiments, Central Guizhou Province**

## 1 Introduction

China is one of the most important countries in the world for her abundant bauxite resources, where there are more than 300 mineral origin places distributed in 19 provinces (regions). And Guizhou is one of the four biggest bauxite resources provinces in China. With its reserves and basic reserves in 155.23 and 216.25 million tons by the end of 2008, Guizhou ranks the first among the four, followed with Henan, Guangxi and Shanxi provinces (Liu et al., 2009; USGS, 2009; Wu et al., 2006). Guizhou bauxite deposits are divided into five bauxite deposit belts, namely, Xiuwen, Xifeng, Zhunyi, Zhengan and Daozhen from south to north. Lindai bauxite, laying in the NWW 32km from the Guiyang city, belongs to Xiuwen bauxite deposit belt. Domestic and foreign scholars have done a lot of researches on bauxite mineralogy and geochemistry and claimed various insights on the genesis of bauxite deposits (Liu et al., 2010; Mongelli, 1997; MacLean et al., 1997; Öztürk et al., 2002; Calagari and Abedini, 2007; Ye et al., 2007; Zhang et al., 2013). Moreover, many researches on the utilization of bauxite associated rare elements have been done as well in recent years and bauxite associated rare elements such as Ga, Li, Sc, Ti and V has achieved industrial grade in many regions and major industrial exploitation value (Tang et al., 2001, 2002; Liu, 2007). But articles in the experimental methods to study the genesis of bauxite deposits are rare, except Valeton (1972) and Chen (1991, 1996) who have done some related experiments and pointed out that the acidic condition is conducive to silicon, aluminum fractionation and that humic acid can enhance the ability of $SiO_2$, $Fe_2O_3$ and $Al_2O_3$ migration as colloidal state in water (Valeton, 1972; Chen, 1991, 1996). By setting the Lindai bauxite deposit in Qingzhen district, Guizhou Province as an example, soaking and leaching the suspected precursor rocks–Shilenshui Formation dolomite and its weathered laterite of the Lindai bauxite by the method of weathering simulation experiments, then contrasting with the different migration relationship of Al, Si, Fe, Ca and Mg. This article will design different pHs as well as a variety of acidic and alkaline conditions to find out the most suitable aqueous conditions for Si and Fe migration but the enrichment of Al. Therefore, we can know the

* Corresponding author. E-mail: zhuxqcas@sohu.com

groundwater conditions to form the bauxite deposits under natural conditions in theory and draw out of the metallogenic model diagram of bauxite in central Guizhou, which can develop basic theory of the bauxite mineralization as well as provide adequate theoretical basis for actual prospecting exploration.

## 2 Geological Setting and Geological Features

The research area is located at Guiyang complex tectonic deformation zone, north Guizhou anticlise, Yangtze paraplatform (Guizhou Provincial Bureau of Geology and Mineral Resources, 1987). In early Paleozoic, most part of Guizhou was in a marine sedimentary environment, and by the end of early Paleozoic, the Caledonian movement has led to central and north Guizhou uplift, forming the central Guizhou doming. It is the large scale ancient complex anticlinal structure which extends northeast, with its structural highs in Zhuzang, Zhijin county, and it is one part of the upper Yangtze ancient land. After nearly 100 million years of weathering and erosion, the central Guizhou has become peneplain landform in Devonian, constituting a favorable basis of geological conditions for the formation of karst type bauxite. At early carboniferous the South China Sea water transgressed from south to north when Lindai area was the karst depression and shallow lake facies, then sedimentation occurred to form the Jiujialu Formation Al-bearing rock series. Moreover, the transgression at Permian extends, and then completely turns central Guizhou into the carbonate deposition at the mid of Qixia epoch (Gao, 1992; Guizhou Provincial Bureau of Geology and Mineral Resources, 1987). Rock units in this region are exposed, including Upper Proterozoic, Sinian, Mid to Upper Cambrian, Lower Carboniferous, Permian and Triassic (Figs. 1a, 1b).

The bauxite is hosted by the Lower Carboniferous Jiujialu Formation, and parallel unconformity with the

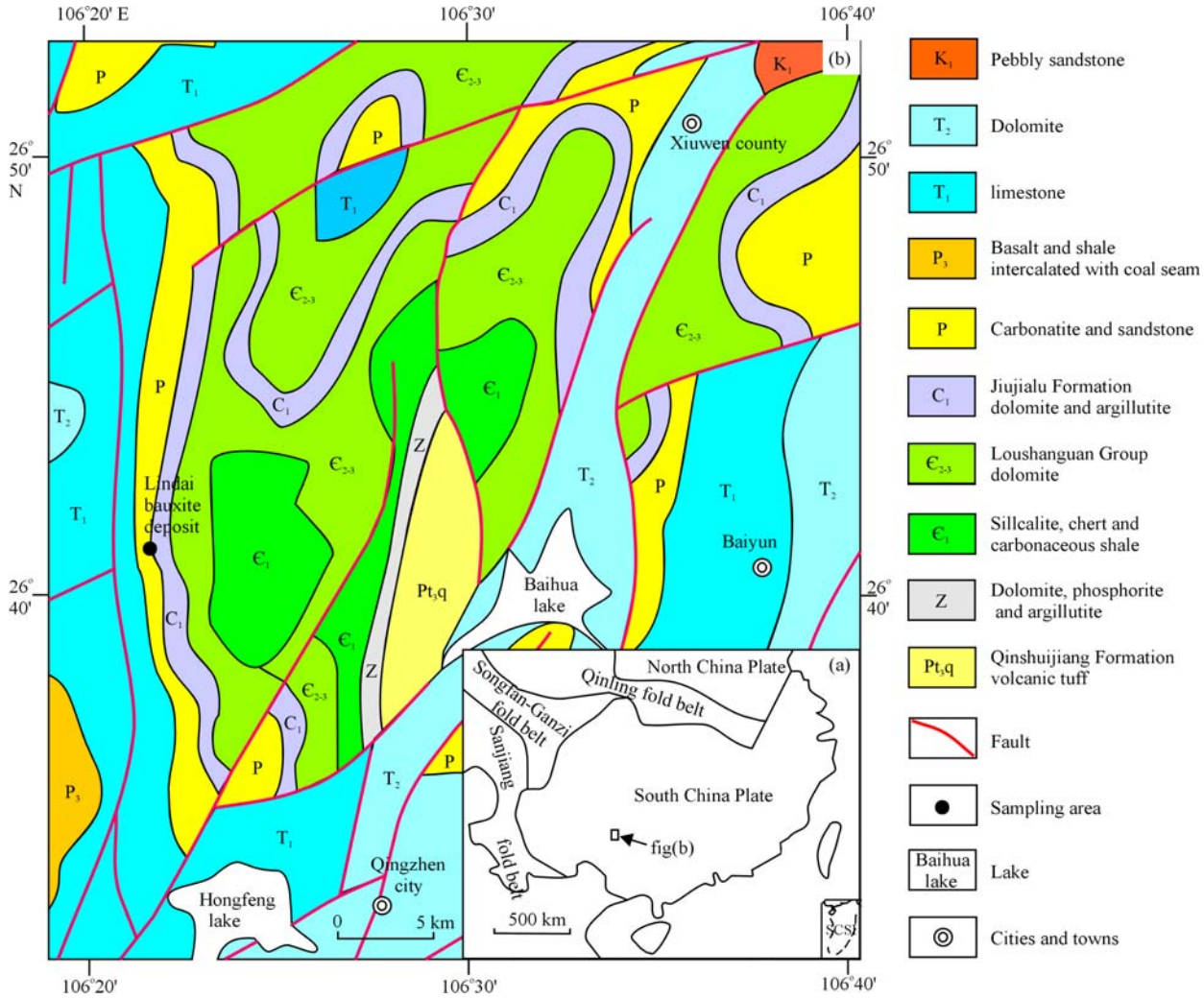


Fig. 1. (a), an index map of South China Plate showing the location of the Lindai bauxite deposit; (b), Geologic map illustrating the geological features of the Lindai bauxite deposit, Guiyang, China.

overlying and underlying strata. The underlying stratum is the Middle Cambrian Shilengshui Formation dolomite while the overlying stratum is the Lower Carboniferous Baizuo Formation dolomite. The geological structure of Qinzhen region is complicated with faults staggered distribution and sequence of strata hybrid. The faults can be divided into two groups, namely, NE and NNE. Ore bearing strata Jiujialu Formation are inverted bedding nearly south-north strike, inclining to NNE with dip angel of 70°–80°. Ore-bearing rock series Jiujialu Formation ($C_1j$) is divided into three layers: the upper layer ($C_1j^3$) is coal beds, composed of black carbonaceous shale intercalated with coal seams, in its thickness of 3–4 m; the middle layer ($C_1j^2$) is bauxite beds, in its thickness of 1–12 m, and 5–6 m in general, consisting of compact bauxite, clastic bauxite and high iron bauxite; the lower layer ($C_1j^1$) is ferruginous beds, mainly ferruginous clay shale and iron ore body, with ferruginous rock composed of red, steel gray or dark clumps of siderites, star dot pyrites and lenses of hematite, in its thickness of 2–10 m (Fig. 2).

## 3 Sampling and Experimental Methods

### 3.1 Sampling

The samples to research were collected from Muzhuchong open pit and outcrop in Lindai bauxite, Qingzhen city. We selected three representative bauxite samples (compact bauxite, clastic bauxite and high iron bauxite) as well as the underlying Shilengshui Formation dolomite and its weathered laterite (Fig. 3). The major element abundances were determined by X-ray fluorescence (XRF) from a panalytical company (formerly Philips Analytical Instruments Division) Model Axios (PW4400) spectrometer. The trace element and rare earth element abundances were analyzed through inductively coupled plasma mass spectrometry (ICP-MS) from a Finnigan MAT company Model ELEMENT. The ICP-OES (Model Vista MPX produced by Varian company) analyses

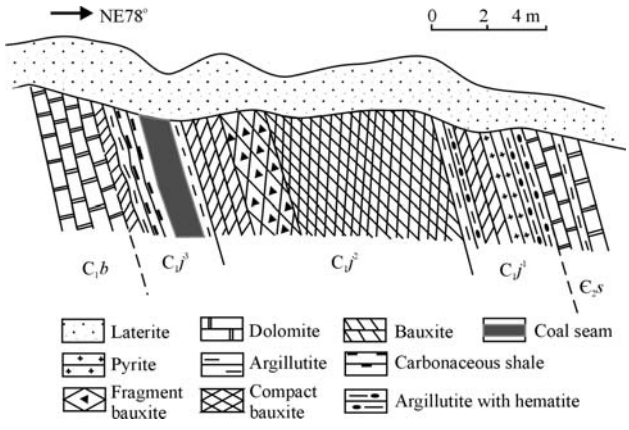


Fig. 2. Geological section of Lindai bauxite deposit.

were utilized for determining the composition of soaking and leaching solution. All of analyses above were determined in Institute of Geochemistry, Chinese Academy of Sciences. The detailed analytical procedures were described by Franzini et al. (1972) and Qi et al. (2000), and the analysis results are summarized in Table 1, 2, 3. The pH values of the solutions were determined by LIDA PHS-3C laboratory pH meter with a rechargeable composite electrode Model E-201-C-9.

### 3.2 Conditional experiments

#### 3.2.1 Soaking experiments

We used the weathering simulation experiment method to soaking the suspected precursor rocks–Middle Cambrian Shilengshui Formation dolomite and its weathered massive laterite of the Lindai bauxite (Fig. 3). Firstly, in the method of tube immersion, with 22 colorimetric tubes of 50 mL for 20–60 mesh samples each in 5 g, add them into the 50 mL prepared solution containing inorganic acid (HCl), organic acid (citric acid) and reducing acid (oxalic acid) for each. Secondly, before closing colorimetric tubes with glass covers, use HCl and NaOH to adjust solution pH to specified values. 30 days later, sampled the solutions with 12 mL. Then, centrifuge and filter the solutions by pinhole filter membrane. Thirdly, before sending these solutions to ICP-OES to be determined, add 0.5 mL of $HNO_3$ to acidify them. Analysis results are summarized in Table 2.

#### 3.2.2 Leaching experiments

Leaching experiments were done with the automatic cycle leaching device (Fig. 4) that is composed of the gas generating device and the automatic cycle leaching device. The latter is composed of three parts, namely, the weathering and leaching, the evaporation cycle as well as the rainwater synthesis. The specific procedures of the experiments are show as follows: (1) Mash the massive laterite and select some 8–20 mesh samples by standard sieve. Before placing them in a 60°C oven thermostat to dry for 8 hours, use running water and then ultrapure water to wash the samples three times respectively. Then weight 130 g laterite samples in three copies by the balance and load them into the glass column at the weathering and leaching part. (2) The $CO_2$-containing gas, HCl-containing gas and air gas produced by generation device goes into the automatic cycle leaching device on the right. (3) Control the power of electric stove to sustain the evaporation at the same level. So water vapor rises up to the rainwater synthesis, mixing with the $CO_2$-containing gas, the HCl-containing gas and the air respectively, and then condensation of three rainwaters with different pH value leaches the sample column at weathering and


Fig. 3. The sample structures in the Lindai bauxite deposit.
(a), Clastic bauxite; (b), compact bauxite; (c), high iron bauxite with star dot pyrite; (d), high iron bauxite with siderite clumps; (e), dolomite and it's weathered massive laterite; (f), dolomite and it's weathered loose laterite.

leaching part. (4) Leaching experiment continues for 15 days with 8 hours a day, about 7 mL leaching solution a minutes. Control the leaching solution to about 2200–2800 mm (divided the total volume of leaching solution by cross-sectional area of sample column), about twice of the annual average rainfall in Guiyang city (1200–1500 mm) (compilation of the annual average rainfall in china with 30 years), which shows that the one day experiments nearly equals to two years weathering and leaching in nature. (5) Sampling the leaching solution 12 mL from the flask every two or three days before constant solution volume to 400 mL. Centrifuge and filter the solutions by Pinhole filter membrane. Before sending these solutions to ICP-OES to be determined, add 0.5 mL of 1:1 $HNO_3$ to acidify. Analysis results are summarized in Table 3.

**Table 1 Major (%), trace and REE (ppm) element compositions of bauxite samples from the Lindai bauxite**

| Sample no | LD-07 | LD-08 | LD-10 | LD-11 | LD-12 | LD-13 | Sample no | LD-07 | LD-08 | LD-10 | LD-11 | LD-12 | LD-13 |
|---|---|---|---|---|---|---|---|---|---|---|---|---|---|
| Lithology | Clastic bauxite | Compact bauxite | High iron bauxite | Loose laterite | Massive laterite | Dolomite | Lithology | Clastic bauxite | Compact bauxite | High iron bauxite | Loose laterite | Massive laterite | Dolomite |
| $SiO_2$ | 1.20 | 34.49 | 1.53 | 36.29 | 40.26 | 2.13 | Sb | 3.66 | 2.04 | 11.7 | 5.37 | 3.09 | 3.97 |
| $Al_2O_3$ | 76.84 | 44.89 | 70.92 | 21.53 | 21.59 | 1.50 | Cs | 0.07 | 2.60 | 0.07 | 18.2 | 28.6 | 0.5 |
| $Fe_2O_3$ | 2.18 | 2.20 | 6.29 | 14.02 | 15.69 | 0.74 | Ba | 8.06 | 33.8 | 8.73 | 258 | 237 | 25.6 |
| MgO | 0.15 | 0.51 | 0.21 | 4.26 | 4.20 | 19.36 | Hf | 51.9 | 32.3 | 33.8 | 6.42 | 14.2 | 0.52 |
| CaO | - | - | - | 2.62 | 0.68 | 29.68 | Ta | 5.19 | 4.81 | 3.76 | 1.56 | 1.76 | 0.28 |
| $Na_2O$ | 0.74 | 0.06 | 1.22 | 0.20 | 0.72 | 0.89 | W | 8.64 | 13.1 | 13.2 | 5.54 | 7.06 | 2.90 |
| $K_2O$ | 0.14 | 1.23 | 0.19 | 5.13 | 6.33 | 0.33 | Tl | 0.03 | 0.09 | 1.15 | 0.80 | 0.67 | 0.05 |
| MnO | - | 0.02 | - | 0.18 | 0.05 | 0.04 | Pb | 158 | 32.6 | 87.8 | 122 | 67.2 | 18.0 |
| $P_2O_5$ | 0.23 | 0.07 | 0.13 | 0.10 | 0.27 | 0.03 | Bi | 8.01 | 3.17 | 2.70 | 0.76 | 0.94 | 0.07 |
| $TiO_2$ | 5.12 | 3.58 | 2.55 | 0.86 | 1.20 | 0.07 | Th | 44.3 | 71.6 | 23.1 | 36 | 32 | 1.65 |
| L.O.I. | 14.31 | 13.46 | 16.97 | 13.73 | 8.03 | 45.24 | U | 48.1 | 14.3 | 54.3 | 7.10 | 6.03 | 0.89 |
| Total | 100.91 | 100.51 | 100.01 | 98.92 | 99.03 | 100.01 | La | 39.1 | 82.8 | 43.5 | 81.0 | 93.3 | 4.64 |
| CIA | 98.87 | 97.22 | 98.05 | 73.03 | 73.62 | 4.63 | Ce | 85.4 | 140 | 44.7 | 164 | 203 | 8.60 |
| Li | 2.63 | 799 | 1.11 | 104 | 94.2 | 6.31 | Pr | 8.98 | 15.4 | 9.03 | 19.0 | 21.0 | 1.13 |
| Be | 6.18 | 3.00 | 5.87 | 8.53 | 5.19 | 0.50 | Nd | 37.8 | 55.3 | 33.1 | 72.0 | 76.6 | 4.55 |
| Sc | 6.68 | 14.7 | 4.64 | 22.7 | 22.7 | 0.77 | Sm | 9.18 | 11.8 | 7.83 | 16.1 | 15.2 | 1.03 |
| V | 138 | 260 | 206 | 129 | 99.0 | 9.91 | Eu | 1.91 | 2.19 | 1.39 | 3.04 | 3.03 | 0.19 |
| Cr | 106.14 | 96.28 | 60.61 | 122.09 | 162.4 | 181.25 | Gd | 13.82 | 11.5 | 17.69 | 15.45 | 14.79 | 1.12 |
| Co | 3.75 | 14.5 | 87.8 | 34.0 | 54.0 | 4.01 | Tb | 2.6 | 1.95 | 3.81 | 2.54 | 2.24 | 0.17 |
| Ni | 210.45 | 103.39 | 144.9 | 170.2 | 297.85 | 225.4 | Dy | 14.1 | 11.8 | 22.2 | 14.8 | 12.1 | 0.99 |
| Cu | 288 | 61.7 | 932 | 36.5 | 20.6 | 32.2 | Ho | 2.58 | 2.49 | 4.10 | 2.86 | 2.41 | 0.18 |
| Zn | 63.7 | 61.3 | 39.6 | 88.7 | 93.1 | 48.4 | Er | 6.99 | 7.74 | 10.5 | 8.46 | 7.12 | 0.49 |
| Ga | 13.9 | 27.3 | 17.2 | 27.1 | 22.5 | 1.37 | Tm | 0.95 | 1.15 | 1.32 | 1.20 | 0.96 | 0.06 |
| Ge | 1.77 | 1.09 | 3.21 | 2.09 | 2.30 | 0.12 | Yb | 5.96 | 7.95 | 7.67 | 8.26 | 6.44 | 0.38 |
| As | 43.0 | 34.8 | 89.0 | 44.9 | 63.3 | 31.1 | Lu | 0.83 | 1.18 | 0.98 | 1.17 | 0.93 | 0.06 |
| Rb | 1.57 | 14.2 | 2.46 | 171 | 153 | 7.38 | ΣREE | 230.2 | 353.26 | 207.82 | 409.89 | 459.12 | 23.58 |
| Sr | 206 | 118 | 52.9 | 68.6 | 85.9 | 85.4 | LREE | 182.37 | 307.49 | 139.55 | 355.14 | 412.13 | 20.14 |
| Y | 71.7 | 56.6 | 116 | 72.9 | 64.4 | 5.35 | HREE | 47.83 | 45.76 | 68.27 | 54.74 | 46.99 | 3.44 |
| Zr | 1890 | 1180 | 1240 | 222 | 512 | 19.3 | LR/HR | 3.81 | 6.72 | 2.04 | 6.49 | 8.77 | 5.85 |
| Nb | 117 | 89.0 | 66.9 | 22.0 | 29.4 | 1.89 | $(La/Yb)_N$ | 4.33 | 6.88 | 3.74 | 6.48 | 9.57 | 8.13 |
| Mo | 6.69 | 1.50 | 13.3 | 4.14 | 11.9 | 4.86 | $(La/Sm)_N$ | 2.61 | 4.30 | 3.40 | 3.08 | 3.76 | 2.76 |
| Ag | 1.65 | 1.19 | 6.07 | 0.27 | 0.37 | - | $(Gd/Lu)_N$ | 2.08 | 1.22 | 2.25 | 1.65 | 1.99 | 2.40 |
| Cd | 0.63 | 0.63 | 0.38 | 0.74 | 0.76 | 0.22 | Ce/Ce* | 1.07 | 0.92 | 0.53 | 0.98 | 1.07 | 0.88 |
| In | 0.32 | 0.37 | 0.18 | 0.13 | 0.15 | 0.01 | Eu/Eu* | 0.52 | 0.58 | 0.37 | 0.60 | 0.63 | 0.54 |
| Sn | 15.9 | 18.2 | 9.44 | 5.05 | 5.33 | 0.51 | La/Y | 0.55 | 1.46 | 0.38 | | | |

Note: $Ce/Ce^*=Ce_N/(La_N \cdot Pr_N)^{1/2}$ ; $Eu/Eu^*=Eu_N/(Sm_N \cdot Gd_N)^{1/2}$

**Table 2 Concentration of soaking solution for dolomite and laterite in the Lindai bauxite (Experiment for 30 days)**

| | Sample number | Characteristic of solution | pH value | Al (ppm) | $SiO_2$ (ppm) | Fe (ppm) | Ca (ppm) | Mg (ppm) | Si/Al | Fe/Al | Ca/Al | Mg/Al | Migration rate of Al (mg/g) | Migration rate of Si (mg/g) | Migration rate of Fe (mg/g) | Migration rate of Ca (mg/g) | Migration rate of Mg (mg/g) |
|---|---|---|---|---|---|---|---|---|---|---|---|---|---|---|---|---|---|
| Dolomite soaking experiment solution | J2-1 | Use HCl and NaOH to adjust pH to specified values | 1.00 | 0.61 | 3.79 | 10.83 | 182 | 56.52 | 2.9 | 17.73 | 298 | 92.51 | 0.77 | 1.78 | 20.75 | 8.59 | 4.87 |
| | J2-2 | | 2.99 | - | 1.24 | 0.02 | 5.71 | 9.06 | - | - | - | - | - | 0.58 | 0.04 | 0.27 | 0.78 |
| | J2-3 | | 5.00 | 0.16 | 0.97 | 0.01 | 2.39 | 3.24 | 2.9 | 0.04 | 15.26 | 20.71 | 0.2 | 0.46 | 0.01 | 0.11 | 0.28 |
| | J2-4 | | 7.00 | - | 1.39 | - | 2.72 | 3.08 | - | - | - | - | - | 0.65 | - | 0.13 | 0.26 |
| | J2-5 | | 9.00 | - | 1.39 | - | 2.53 | 2.94 | - | - | - | - | - | 0.65 | - | 0.12 | 0.25 |
| | J2-6 | | 10.99 | 0.02 | 2.29 | 0.01 | 2.82 | 1.90 | 54.07 | 0.34 | 142 | 96.21 | 0.02 | 1.07 | 0.01 | 0.13 | 0.16 |
| Massive laterite Soaking experiment solution | J2-7 | Use HCl and NaOH to adjust pH to specified values | 1.00 | 73.65 | 86.73 | 20.75 | 119 | 40.39 | 0.55 | 0.28 | 1.62 | 0.55 | 6.44 | 2.15 | 1.89 | 244 | 16.03 |
| | J2-8 | | 3.00 | 0.05 | 3.64 | 0.04 | 6.59 | 6.08 | 34.28 | 0.87 | 133 | 122 | 0.01 | 0.09 | 0.01 | 13.49 | 2.41 |
| | J2-9 | | 5.01 | 0.22 | 2.1 | 0.14 | 2.75 | 3.49 | 4.48 | 0.64 | 12.58 | 15.93 | 0.02 | 0.05 | 0.01 | 5.63 | 1.38 |
| | J2-10 | | 7.01 | 2.72 | 7.2 | 1.46 | 7.28 | 3.15 | 1.23 | 0.54 | 2.67 | 1.16 | 0.24 | 0.18 | 0.13 | 14.9 | 1.25 |
| | J2-11 | | 9.00 | 0.79 | 3.61 | 0.46 | 4.17 | 4.21 | 2.14 | 0.59 | 5.30 | 5.35 | 0.07 | 0.09 | 0.04 | 8.54 | 1.67 |
| | J2-12 | | 11.00 | 2.51 | 6.21 | 1.34 | 6.43 | 2.33 | 1.16 | 0.54 | 2.57 | 0.93 | 0.22 | 0.15 | 0.12 | 13.16 | 0.93 |
| | J2-13 | Add 0.5 g oxalic acid then adjust pH to specified values | 1.49 | 355 | 195 | 89.34 | 169 | 49.57 | 0.26 | 0.25 | 0.48 | 0.14 | 31.04 | 4.83 | 8.13 | 345 | 19.67 |
| | J2-14 | | 3.00 | 105 | 95.76 | 217 | 85.39 | 26.7 | 0.42 | 2.06 | 0.81 | 0.25 | 9.23 | 2.38 | 19.76 | 174 | 10.59 |
| | J2-15 | | 4.99 | 8.16 | 9.53 | 5.39 | 8.49 | 32.69 | 0.55 | 0.66 | 1.04 | 4.01 | 0.71 | 0.24 | 0.49 | 17.38 | 12.97 |
| | J2-16 | | 7.00 | 2.98 | 3.47 | 0.70 | 2.86 | 30.04 | 0.54 | 0.24 | 0.96 | 10.08 | 0.26 | 0.09 | 0.06 | 5.85 | 11.92 |
| | J2-17 | | 9.00 | 1.97 | 6.78 | 1.01 | 6.29 | 28.5 | 1.61 | 0.51 | 3.19 | 14.46 | 0.17 | 0.17 | 0.09 | 12.87 | 11.31 |
| | J2-18 | Add 0.5 g citric acid then adjust pH to specified values | 2.18 | 60.9 | 61.51 | 21.21 | 71.82 | 27.49 | 0.47 | 0.35 | 1.18 | 0.45 | 5.33 | 1.53 | 1.93 | 147 | 10.91 |
| | J2-19 | | 3.00 | 51.84 | 40.62 | 24.24 | 45.13 | 23.66 | 0.37 | 0.47 | 0.87 | 0.46 | 4.54 | 1.01 | 2.21 | 92.36 | 9.39 |
| | J2-20 | | 5.01 | 25.83 | 28.64 | 15.49 | 44.16 | 30.4 | 0.52 | 0.6 | 1.71 | 1.18 | 2.26 | 0.71 | 1.41 | 90.4 | 12.06 |
| | J2-21 | | 7.01 | 16.09 | 24.12 | 10.12 | 40.09 | 28.49 | 0.7 | 0.63 | 2.49 | 1.77 | 1.41 | 0.6 | 0.92 | 82.05 | 11.31 |
| | J2-22 | | 9.01 | 15.57 | 21.68 | 9.88 | 41.73 | 28.92 | 0.65 | 0.63 | 2.68 | 1.86 | 1.36 | 0.54 | 0.90 | 85.4 | 11.48 |

### 3.2.3 Method of data processing

Because we used continuous sampling method and sampled a large amount volume of solution from flask, we converted the data to make the experiments more accurate. All data this article mentioned are the result of conversion. The convert method explain as follows: assuming first, second, third sampling…, and concentrations of element a are $a_1$, $a_2$, $a_3$…mg/L respectively, so the net contents of element a in select samples are $v{\cdot}a_1$, $v{\cdot}a_2$, $v{\cdot}a_3$…mg respectively, now the conversion concentrations of soaking and leaching solutions are $a_1$, $(V{\cdot}a_2+v{\cdot}a_1)/V$, $(V{\cdot}a_3+v{\cdot}a_2+v{\cdot}a_1)/V$…mg/L respectively. The V (L) is the total volume of the soaking or leaching solutions and v (L) is the volume of the select samples.

The method of element migration rate ($K_x$) calculation is referred and improved to the formula from Chen and Zhu (1984):

$K_x = (a_x{\cdot}V)/A_x{\cdot}M$ or $K_x = (a_x{\cdot}V) \cdot 1000 / A_x{\cdot}M$

Ax is the concentration of the soaking of leaching solutions(ppm); V is the total volume of the soaking or leaching solutions (L); $A_x$ is the abundance (wt%) of the elements in rock sample; M is the weight (g) of the rock sample. The physical meaning of element migration rate ($K_x$) is the mg or μg number of the elements migration by the soaking or leaching solutions during the experiment in 1000 g sample, if every element is just 1 g.

## 4 Results and Discussions

### 4.1 Major elements geochemistry

The $Al_2O_3$ contents in three different types of bauxite vary from 44.89 wt% to 76.84 wt%; the $Fe_2O_3$ content in high iron bauxite reached as much as 6.29 wt%, and another two are 2.18 wt% and 2.20 wt% respectively (Table 1). The ferriferous minerals in high iron bauxite are mainly star dot pyrite, siderite clumps (Figs. 3c, 3d) and a little bit of epigenetic oxidation of hematite and goethite, which indicate that the Lindai bauxite deposit was formed with the reducing environment (Butler and Rickard, 2000; Zarasvandi et al., 2008). The concentrations of $SiO_2$ in LD-7 and LD-10 are as low as only 1.20 wt% and 1.53 wt% respectively, but it is as much as 34.49 wt% in LD-8. This may be the result of the more contents of clay minerals such as kaolinite (Mameli et al., 2007). The contents of Ti are higher than the usual ones, which might be formed the alteration of micas mineral, such as biotite, or from clay minerals with high Ti contents (Öztürk, 2002).

The chemical indexes of alteration (CIA) (Nesbitt and Young, 1982) of all the three bauxites are over 97, which means that the source rock had undergone a complete process of weathering, whereas the two laterite sample's CIA are just around 73, which means it have not been

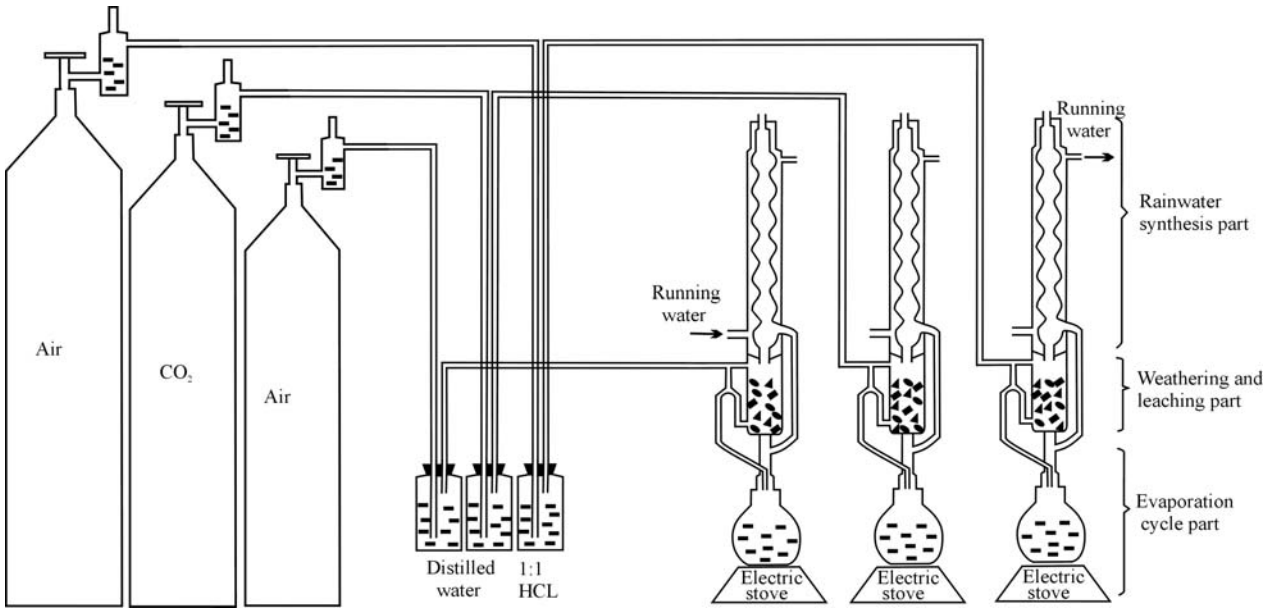


Fig. 4. Schematic diagram of leaching device.

**Table 3 Concentration of leaching solution for laterite in the Lindai bauxite**

| Characteristic of solution | Sample number | Experiment Times (d) | Al (ppm) | Fe (ppm) | $SiO_2$ (ppm) | Si/Al | Fe/Al | pH values | Migration rate of Al (μg/g) | Migration rate of Fe (μg/g) | Migration rate of Si (μg/g) |
|---|---|---|---|---|---|---|---|---|---|---|---|
| Air leaching solution with pH=7.00 | Air-1-2 | 1 | 0.53 | 0.34 | 68.1 | 60.2 | 0.64 | 6.47 | 14.2 | 7.24 | 400 |
| | Air-2-2 | 3 | 0.67 | 0.41 | 130 | 89.9 | 0.6 | 6.46 | 18.2 | 8.79 | 763 |
| | Air-3-2 | 6 | 0.06 | 0.05 | 124 | 897 | 0.83 | 7.63 | 1.73 | 1.15 | 727 |
| | Air-4-2 | 9 | 0.07 | 0.04 | 177 | 1180 | 0.64 | 7.72 | 1.88 | 0.96 | 1039 |
| | Air-5-2 | 12 | 0.06 | 0.06 | 130 | 1098 | 1.01 | 9.03 | 1.48 | 1.19 | 763 |
| | Air-6-2 | 15 | 0.08 | 0.06 | 190 | 1103 | 0.72 | 9.27 | 2.16 | 1.24 | 1115 |
| $CO_2$ leaching solution with pH=5.11 | CO2-1-2 | 1 | 0.01 | 0.01 | 51.7 | 1772 | 0.54 | 8.07 | 0.37 | 0.16 | 304 |
| | CO2-2-2 | 3 | 0.01 | 0.01 | 88.2 | 3923 | 0.73 | 7.98 | 0.28 | 0.17 | 518 |
| | CO2-3-2 | 6 | 0.01 | 0.01 | 124 | 5406 | 1.09 | 7.82 | 0.29 | 0.25 | 732 |
| | CO2-4-2 | 9 | 0.01 | 0.01 | 118 | 2124 | 2.99 | 7.95 | 0.07 | 0.17 | 697 |
| | CO2-5-2 | 12 | 0.01 | 0.01 | 116 | 6830 | 0.69 | 7.68 | 0.21 | 0.12 | 684 |
| | CO2-6-2 | 15 | 0.02 | 0.01 | 124 | 3593 | 0.55 | 8.21 | 0.43 | 0.19 | 730 |
| HCl leaching solution with pH=3.48 | HCl-1-2 | 1 | 0.01 | 0.01 | 37.6 | 6518 | 3.41 | 7.62 | 0.07 | 0.20 | 221 |
| | HCl-2-2 | 3 | 0.01 | 0.01 | 80.9 | 9356 | 0.68 | 7.35 | 0.11 | 0.06 | 476 |
| | HCl-3-2 | 6 | 0.02 | 0.01 | 112 | 2282 | 0.44 | 7.5 | 0.62 | 0.22 | 661 |
| | HCl-4-2 | 9 | 0.05 | 0.01 | 129 | 1296 | 0.21 | 7.38 | 1.25 | 0.21 | 756 |
| | HCl-5-2 | 12 | 0.68 | 0.27 | 192 | 133 | 0.39 | 5.36 | 18.2 | 5.74 | 1129 |
| | HCl-6-2 | 15 | 0.19 | 1.13 | 262 | 646 | 5.95 | 4.84 | 5.10 | 24.29 | 1540 |

fully weathered and is still undergoing the weathering process at the time. At last, classifying the bauxites by Ki index [Ki= $(SiO_2/Al_2O_3))\times1.78$] (Al-Bassam, 2005), the Ki values of LD-7, LD-10 and LD-8 are 0.03, 0.01 and 1.37 respectively, which indicate that LD-7 and LD-10 are the high quality bauxite while LD-8 is the bauxite clay.

### 4.2 Rare earth (REE) and trace elements geochemistry

#### 4.2.1 Rare earth element (REE) geochemistry

Rare earth element (REE) geochemistry data (Table 1) indicate that the ΣREE (23.58–459.12 ppm, average 280.65 ppm) varied widely, with LREE significant enrichment and Eu medium depletion, except dolomite. LREE/HREE values 2.04–8.77 while $(La/Yb)_N$, $(La/Sm)_N$ and $(Gd/Lu)_N$ values 3.74–9.57, 2.61–4.30 and 1.22–2.40 respectively. REE patterns are the right curve (Fig. 5a) with the patterns of the three bauxites and two laterites are similar to the underlying dolomite. Moreover, in contrast to the dolomite, HREE and LREE are strongly enriched, with their curve patterns similar to the dolomite ones as well. The analyses above indicate that the same source of rock that bauxites and laterites share might be the underlying Shilengshui Formation dolomite. And the weathering laterite is the in-process products from mother rock to the bauxite.

The ΣREE, LREE and LREE/HREE values of massive bauxite LD-8 (bauxite clay) are the highest of the three bauxites. It might be caused by the different effect on the rare earth elements absorption for clay minerals. Also, contents of clay minerals are positive correlations to the

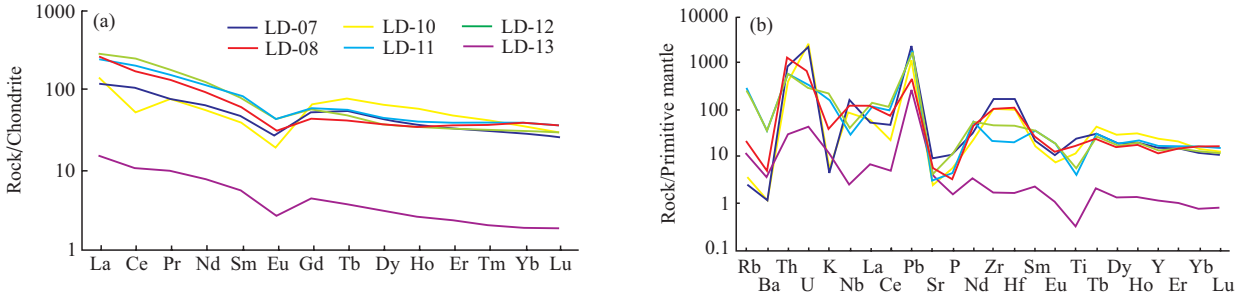


Fig. 5. Chondrite-normalized REE patterns (a) and primitive mantle-normalized trace element patterns (b) of samples in Lindai bauxite (after Masuda et al., 1973; McDonough et al., 1992).

values of ΣREE. The absorption energy of $REE^{3+}$ is related to the size of the ionic radius and would increase in ascending order from La-Ce to Yb-Lu with the decrease in ironic size (Ye et al., 2007). So massive bauxite rich in clay minerals LD-8 (bauxite clay) is enrich ΣREE, LREE with higher LREE/HREE values. The Ce is medium depletion in the high iron bauxite (LD-10) with the equation $Ce/Ce^*=2Ce_N/(La_N \cdot Pr_N)$ (Taylor and McLennan, 1985; Abedini and Calagi, 2013) and $Ce/Ce^*$ values 0.53 because Ce is price change element and it have two price, $Ce^{3+}$ and $Ce^{4+}$. $Ce^{3+}$ is more easily migrated by groundwater than $Ce^{4+}$ because it is more active. Therefore, Ce mainly exists in the form of $Ce^{3+}$ in reducing environment and significant migration of $Ce^{3+}$ resulted in Ce depletion.

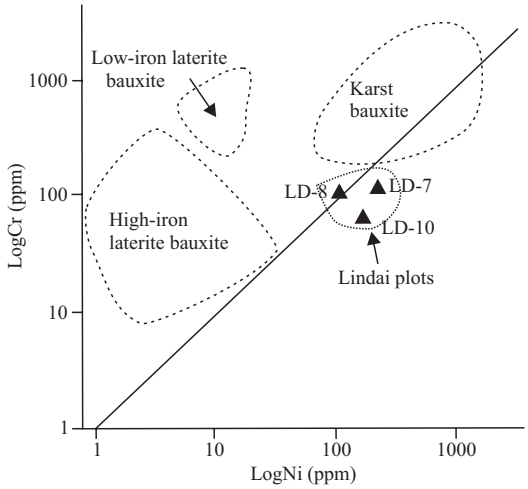


Fig. 6. Plot of Ni vs. Cr concentration for various types of bauxite (after Schroll and sauer, 1968).

### 4.2.2 Trace element geochemistry

Trace element patterns of the two laterite samples are similar to the ones of dolomite (Fig. 5b). But only Sr depletion takes place because Sr, as a large ion lithophile element, could easily dissolve in water and has active geochemical properties. So in the process of weathering, it could be easily migrated by groundwater to the open sea at last, which is the reason why Sr contents are higher in marine sediments than those in continent sediments as well. Spider diagram of three bauxite samples are also similar to the dolomite (Fig. 5b) with Rb, Ba, Sr and a few other elements anomaly. This is because bauxites have processed the more complex stage of diagenic and epigenetic changes while laterites have not. All above indicate that the bauxites and laterites have the inheritance relationship with the dolomite.

In Plot of Ni vs. Cr concentration (Schroll and Sauer, 1968), the bauxite sample plots are close to karst type bauxite area (Fig. 6). It indicates that the bauxite deposit should belongs to karst type bauxite (sedimentary type or paleo-laterite type) though there are some deviation of the sample plots caused by the epigenetic weathering and leaching effects (Ling et al., 2013). The La/Y values are 0.55 for LD-7, 0.38 for LD-10 and 1.46 for LD-8 respectively, which shows that the first two high quality bauxites were formed in acid environment and the forming of high iron bauxite (LD-10) had lower pH values. However, the $Al_2O_3$ content for bauxite clay is just 44.89 wt%, which means that it was formed in alkaline environment (Crnicki and jurkovic, 1990; Maksimovic and Panto, 1991). It just indicates that bauxite mineralization progress of Si, Fe removal and Al enrichment required acid conditions (low pH values).

### 4.3 Condition experimental discuss

### 4.3.1 Leaching experiments

The concentration of the Si can be achieved to 200 ppm but the concentrations of Al and Fe be less than 1ppm on massive laterite leaching experiment (Fig. 7). It means Si could be easily transported but Fe and Al be difficult to migrated. Therefore, Fe migration becomes the key of bauxite formation. However, Fe migration is as difficult as Al under natural conditions, so only in some special environment could the high quality bauxite be formed with Fe removed and Al remained. Although the concentrations of those three elements might not be the highest in acid leaching solution at the beginning, the experiment with pH=3.48 leaching solution had the highest element concentration as the experiment

progresses (Figs. 7a, 7b, 7c), and the abnormal of the element concentrations might be the results of the flushing effects on samples by leaching solution at the beginning of the experiments. The leaching experiments shows that migration rates of Al, Si and Fe in acid condition are higher than that in neutral conditions. But the migration rate of Al in strong acid condition of pH=3.48 is 10 to 20 times higher than that in neutral condition (Table 3), so significant migration of Al makes against the formation of the bauxite obviously. As a result, it is not conducive to form high quality bauxite with the strong acidic conditions in bauxite mineralization process.

The graph of Values of Si/Al and Fe/Al for massive laterite leaching solutions (Fig. 8) could explain the question of Al migration conditions. In the later stage of the experiments, values of Si/Al in leaching solution with condition of pH=5.11 and 7.00 are larger than those with pH=3.48 (Fig. 8a), which means neutral and weak acidic conditions are conductive to Si removal and Al enrichment. The leaching solution with condition of pH=3.48 has the highest Fe/Al value (Fig. 8b), showing that strong acid condition is good for Fe removal and Al enrichment. However, the migration rate of Al is also high in strong acid condition, which obviously shows that significant migration of Al will not be good for high quality bauxite formation. All above suggest that the mineralization of bauxite is a complex process, and require a relatively strict pH conditions. Neutral and weak acidic conditions are conductive to Si removal and Al enrichment, but not good for Fe removal, so the high iron low quality bauxite formed at last; strong acid conditions may be easy for Fe removal but difficult for Si removal, so the high silicon low quality bauxite formed. In conclusion, in the forming process of bauxite, it must experience one or more times changes in pH cycles, from neutral and weak acidic to strong acid or reverse, thus it can make Si, Fe removed and Al enriched to form the high quality bauxites.

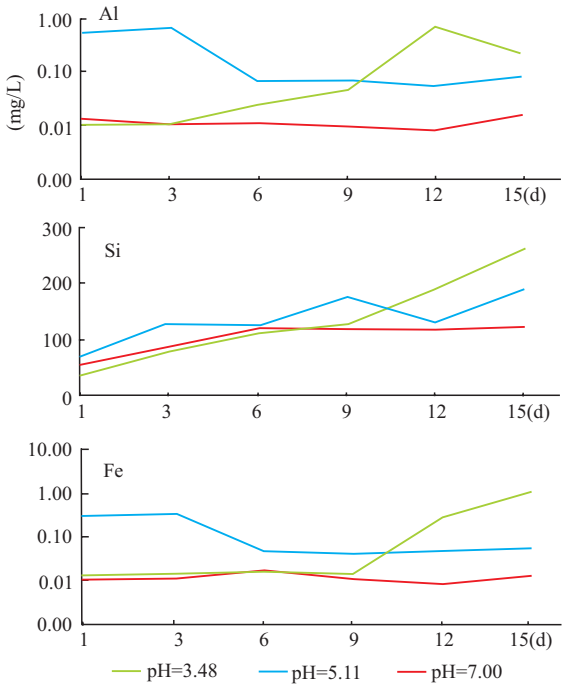


Fig. 7. Concentration of Al, Si, Fe for massive laterite leaching experiments.

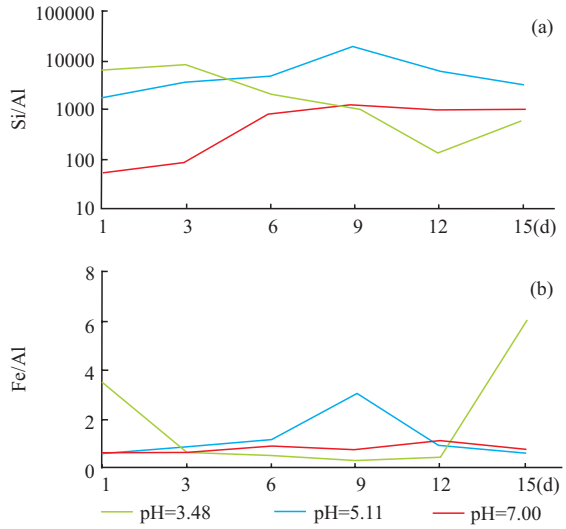


Fig. 8. Values of Si/Al (a) and Fe/Al (b) for massive laterite leaching experiments.

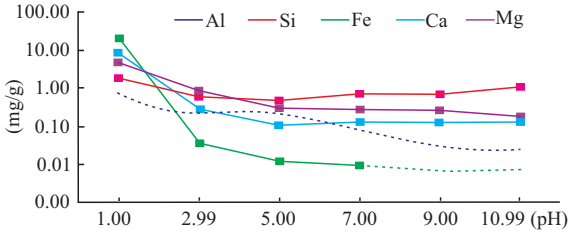


Fig. 9. Migration rate of each element for Dolomite soaking experiments (The dotted lines are speculated).

### 4.3.2 Soaking experiments

In dolomite soaking experiments, the elements migration rates (activity) in natural condition (pH=3.00–9.00) ordered from high to low: Si>Mg>Ca>Al>Fe. In strong acid (pH=3.00–1.00) conditions (Fig. 9), the migration rate of five elements obviously increased, and some even increased several orders of magnitude, among which Fe changed most.

In massive laterite soaking experiments with different pH and Eh values, the order of elements migration rates (activity) changed in natural conditions (pH=3.00–9.00) in contrast to the dolomite: Ca>Mg>Si>Al>Fe. The orders of Ca, Mg and Si changed except Al and Fe (Fig. 10a). The migration rate of Si is higher than that of Mg and Ca; this may be caused by the higher concentration of MgO and CaO in dolomite than massive laterite, which led to Mg

and Ca oversaturated precipitation affecting the migration rates. At the filtration process for dolomite soaking solution, we filtered out a lot of white sediments. In order to identify the main components of the sediment substances, the authors did chemical experiments as followed: first, dried the white sediments by the oven thermostat; second, instilled dilute hydrochloric acid to the sediments, and most dissolved and produced large amounts of colorless, odorless gas. Third, divided the solution into two parts, one was to instill the NaOH solution and it appeared white sediment $Mg(OH)_2$, while the other was to instill the $BaCl_2$ solution and it appeared white sediment $BaSO_4$. So, the authors speculate that the white sediments in dolomite soaking solutions are carbonate and sulfate of Ca and Mg.

In laterite soaking experiments with reducing acid (oxalic acid) in pH≤5.00, migration rate of Al and Fe in solutions are much higher than those without reducing acid (oxalic acid) (Fig. 10b). It suggests that acid and reducing condition can strongly promote Fe and Al migration. And the migration of five elements in solutions with organic acid (citric acid) obviously increased and with the gentle curve (Fig. 10c), which suggest that the organic acid can strongly promote the migration of the five elements. It probably resulted from the organic acid complexes with five elements that promote the elements to be dissolved and migrated. For a single element, the gentle concentration curve may be the small effect of elements migration rate from changes of pH values and the strong effect of the organic acid, which indicate that the effect of organic acid conditions on promoting elements migration rate is much better than that of pH value conditions.

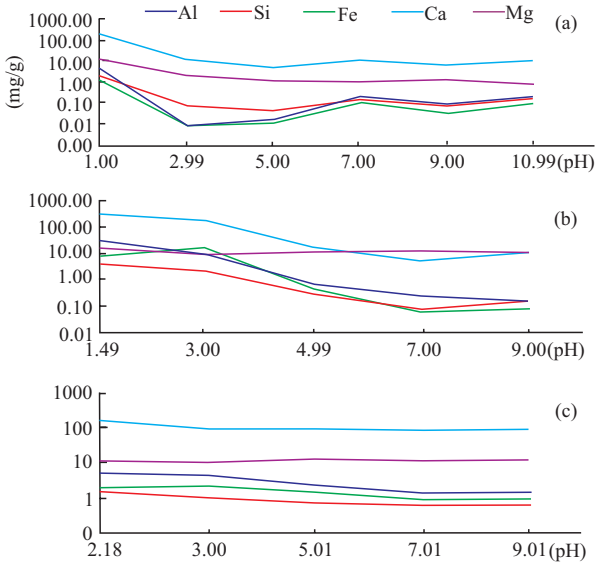


Fig. 10. Migration rate of each element for massive laterite soaking experiments with HCl (a), oxalic acid (b), citric acid (c).

The values of migration rate of Si division by migration rate of Al ($K_{Si}/K_{Al}$) are higher in soaking experiment solutions with inorganic acid than those with reducing acid and organic acid. Furthermore, the Si/Al values are all more than 1 in pH=3.00–9.00, and reached as high as 20.86 in pH=3.00 (Fig. 11a). It means that it is conductive to Si removal and Al enrichment under natural condition with no reducing substance, and the neutral and weak acid with non-reducing condition is the best. However, Fe/Al values are different. Only in the condition of pH=3.00 the $K_{Fe}/K_{Al}$ value is over 1 and reached 2.14. Besides, it is only 0.2–0.4 in strong acid (pH=1.00) condition (Fig. 11b). It shows that the migration rate of Al is higher than that of Fe in strong acid condition, and is obviously not good for bauxite formation, of which the conclusion is the same with massive laterite leaching experiment. All above, the conditions of Fe removal from high aluminum laterite to form bauxite are strict. Only in acid and reducing environment can make Fe removal and Al enrichment. Because of this, many bauxite mines have the high iron bauxite (red ore) around the world, such as Zagros bauxite in Iran, west Jiyuan bauxite in Henan Province, Xiaoshanba bauxite in Guizhou province (Zarasvandi et al., 2008; Chen, 2007; Ye et al., 2007). And the research area also has the high iron bauxite as well, such as the sample LD-10 (Figs. 3c, 3d). Overall, its average grade and quality are not as good as low iron bauxite.

## 5 Metallogenic Model

According to the conclusion through weathering simulation experiments, we propose the metallogenic

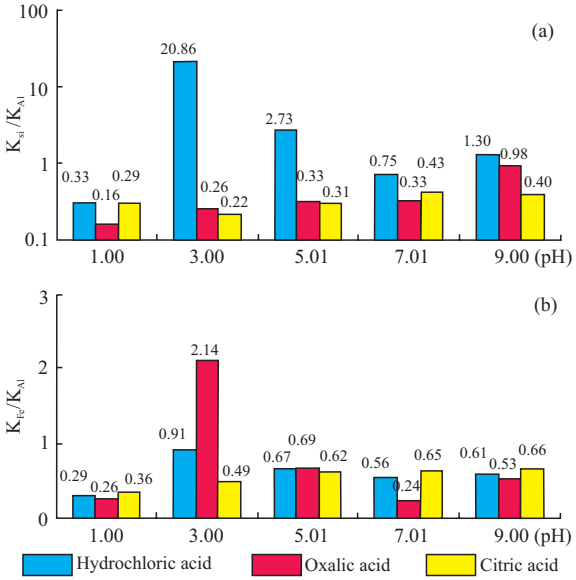


Fig. 11. Values of $K_{Si}/K_{Al}$ (a) and $K_{Fe}/K_{Al}$ (b) for massive laterite soaking experiments.

model of bauxite in central Guizhou province (Fig. 12):

(1) The central and north Guizhou was uplift to land by the late Paleozoic Caledonian movement, and then processed razed denudation and peneplane for almost 100Ma which led this area to missing Devonian, Silurian and Ordovician stratum. Until Al-bearing rock series deposit at early carboniferous, central Guizhou old land had formed a quasi-lysogenic landform which widely distributed of karst depressions and catchment basin, having formed the favorable place for bauxite deposit (Gao et al., 1992).

(2) According to the paleomagnetic remanence analysis, Guizhou area, located at south latitude 8–14 degrees in carboniferous (Liu et al., 1990), belonged to the hot and humid tropical climate and conducive to forming the laterite weathering crust, which provided the necessary climate conditions for the Guizhou bauxite formation. After intense weathering in tropical humid climate of Middle Cambrian Shilengshui Formation impure carbonate rock, K, Na, Ca, Mg and other active elements were moved out while Fe, Al, Ti, Si and other inactive elements were remained in paleo-weathering crust to form the aluminum-rich laterite. Then with the invasion of South China Sea water from south to north at early carboniferous, aluminum-rich laterite or situ or transported to karst depression, catchment basin or doline funner by surface runoff and marine transgression, deposition to form the "original bauxite material", the precursor of bauxite. Lindai bauxite was the product of paleo-laterite deposited in "Xiuwe, Qingzhen karst depression" (Gao et al., 1992).

(3) Tropical humid and hot climate led to lush vegetation on lands, and a large amount of plants decomposition to produce humid acid flowed towards high aluminum laterite deposit area such as closed and semi-closed karst depressions. As a result, the neutral or weak acid environment formed and it provided the favorable environment conditions for Si removal and Al enrichment. Moreover, the more closed the basin was, the more conductive it was to maintain water acidic property, and to have the "original bauxite material" alteration with Si removal and Al enrichment in acidic or weak acidic conditions (nature with unreduced conditions) (Wang et al., 2011).

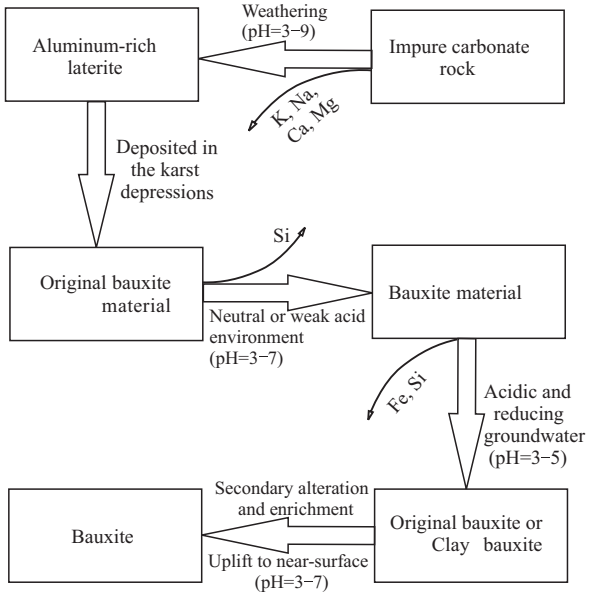


Fig. 12. The metallogenic model diagram of bauxite in central Guizhou province, China.

(4) After the investigation and researched for carboniferous Jiujialu Formation Al-bearing rock series in central Guizhou Province, Permian Liangshan Formation Al-bearing rock series in north Guizhou Province, Permian Heshan Formation Al-bearing rock series in Guangxi Province, Carboniferous Benxi Formation and Permian Wujiaping Formation Al-bearing rock series inYunnan Province Al-bearing rock series, we found that bauxite beds are often accompanied with the rich iron beds and coal beds, constituting a "coal-bauxite-iron" special structure, which is also widespread in foreign deposits such as Ghiona bauxite deposit in Greece, Nurra bauxite deposit in Italy, Kanisheeteh bauxite deposit in Iran (Kalsitzidis et al., 2010; Mameli et al., 2007; Calagari and Abedini, 2007; Zhang et al., 2012). After the long term of Al enrichment and Si removal, the "original bauxite material" developed into "bauxite material" with a lower Si contents (<20 wt%). Afterwards it deposited the organic-rich sediments at the top of the bauxite beds which were precursor of the "coal" of "coal-bauxite-iron" structure. Because the pyrite and other sulfide in "coal" could be easily oxidized, the acidic and reducing groundwater($H_2S$, $H_2SO_4$, etc.) it produced percolated downwards, resulting in bleaching and Al enrichment of the upper part of the underlying bauxite (Kalsitzidis et al, 2010). It also could reduce $Fe^{3+}$ to the easily migrated $Fe^{2+}$ and transport it down near the basal carbonate to make precipitations of the "iron" ($FeS_2$, $FeCO_3$, etc.) of the "coal-bauxite-iron" structure. Thus, after the Fe removed and further removed of the Si for the bauxite material, the "original bauxite" or clay bauxite formed in a certain geological period. Research and studies have shown that it is the positive correlation between the thickness of Lower Carboniferous Jiujialu formation Al-bearing rock series in central Guizhou Province and lower segment "Qingzhen-type iron deposit". The thicker bauxite beds were, the thicker ferruginous rocks were; the thinner bauxite beds were, the thinner ferruginous rocks were or absent (Yang et al., 2011). This can be better shown that bauxite beds are close link with the lower segment ferruginous rocks

that the thicker bauxite beds are, the more $Fe^{2+}$ were transported down to the lower segment by acidic and reducing groundwater and then the thicker ferruginous rocks formed.

(5) Guizhou area experienced the crust uplift at late Triassic and had its conversion from sea to land after all the sea water regressed till Rhaetia (Guizhou Provincial Bureau of Geology and Mineral Resources, 1987). Then the later Tectonic movements uplift the "original bauxite" or clay bauxite to near-surface, so the coal beds or carbonaceous shale continued to produce the acidic and reducing groundwater to have secondary alteration and enrichment for the "original bauxite" or clay bauxite, which ultimately formed the high quality bauxite available to industrial exploitation.

## 6 Conclusions

(1) The source rock of Lindai bauxite may be the underlying Shilengshui Formation dolomite and the weathering laterite is the in-process products from mother rock to the bauxite.

(2) Weathering simulation experiments (leaching experiment and soaking experiment) show that the neutral and acid non-reducing condition is the most conducive to the Al rich and Si removal, and the acid reducing conditions is the most conducive to the Al rich and Fe removal.

(3) During the process of bauxite formation, Coal beds or other rock formation rich in organic material overlying the Al-bearing rock series produce acid reducing groundwater which may be important for bauxite mineralization.

(4) Propose the metallogenic model of bauxite in central Guizhou Province (Fig. 12) and put forward three new words which are "original bauxite material", "bauxite material" and "original bauxite". "Original bauxite material" is the precursor substances of bauxite which transition from the aluminum-rich laterites after it were deposited in karst depressions or catchment basins. "Bauxite material" which with a lower Si contents (<20 wt%) is the product of desilication of "Original bauxite material". And "original bauxite" is the bauxite or clay bauxite which haven't uplifted to near-surface.

## Acknowledgements

This work was granted by the fund of State Key Laboratory of Ore Deposit Geochemistry (SKLODG-ZY125-01) and the Major Project of Chinese National Programs for Fundamental Research and Development (973 Program)(No. 2014CB440906 and 2012CB416602). The author is grateful to two reviewers for their questions and detail guidance to this paper, thanks researcher Liu Jiaren and Chen Wei for the help of field geological investigation, and would like to thank researcher Sheng Zhangqi for his guidance and assistance as well.

Manuscript received Mar. 26, 2013
accepted Aug. 6, 2013
Edited by Liu Lian

### References

Abedini, A., and Calagari, A.A., 2013. Rare earth elements geochemistry of Sheikh-Marut laterite deposit, NW Mahabad, West-Azarbaidjan Province, Iran. *Acta Geologica Sinica* (English Edition), 87(1): 173–185.

Al-Bassam, K.S., 2005. Mineralogy and geochemistry of the Hussainiyat karst bauxite and Zabira stratiform bauxite in northern Arabian Peninsula. *Iraqi Bulletin Geology and Mining*, 1(2): 15–44.

Bureau of Geology and Mineral Resources of Guizhou Province, 1987. *Regional Geology of Guizhou Province*. Beijing: Geological Publishing House, 555–557 (in Chinese).

Butler, I., and Rickard, D., 2000. Framboidal pyrite form ation via the oxidation of iron (Ⅱ) monosulfide by hydrogen sulphide. *Geochimica et Cosmochimica Acta*, 64: 2665–2672.

Calagari, A.A., and Abedini, A., 2007. Geochemical investigations on Permo-Triassic bauxite horizon at Kanisheeteh, east of Bukan, West-Azarbaidjan, Iran. *Journal of Ceochemical Exporation*, 94: 1–18.

Chen Fu and Zhu Xiaoqing, 1984. Simulating expriments on the mechanism of formation of banded iron-silica formations: Weathering–leaching of basalts. *Geochimica*, 4: 341–349 (in Chinese with English abstract).

Chen Lu'an, 1991. Experimental research of elemental differentiations in the forming process of bauxite. *Acta Sedimentologica Sinica*, 9(4): 87–95 (in Chinese with English abstract).

Chen lu'an, 1996. Experimental study of action of humic acids in the processes of bauxite mineralization. *Acta Sedimentologica Sinica*, 14(2): 117–123 (in Chinese with English abstract).

Chen Wang, 2007. Ore-forming conditions of bauxite deposits in west Jiyuan Henan. *Geology and Prospecting*, 43(1): 26–31 (in Chinese with English abstract).

Crnicki, J., and Jurkovic, I., 1990. Rare earth elements in Triassic bauxites of Croatia Yugoslavia. *Travaux*, 19: 239–248.

Franzini, M., Leoni, L., and Saitta, M., 1972. A simple method to evaluate the matrix effects in X-ray fluorescence analysis. *X-Ray Spectrom*, 1: 151–154.

Gao Daode, Sheng Zhangqi, Shi Shanhua and Chen Lu'an, 1992. *Studies on the Bauxite Deposit in Central Guizhou, China*. Guiyang: Guizhou Science & Technology Publishing House, 11–20 (in Chinese).

Kalaitzidis, S., Siavalas, G., Skarpelis, N., Araujo, C.V., and Christanis, K., 2010. Late Cretaceous coal overlying karstic bauxite deposits in the Parnassus-Ghiona unit, central Greece: Coal characteristics and depositional environment. I*nternational Journal of Coal Geology*, 81: 211–226.

Khanehbad, M., Moussavi-Harami, R., Mahboubi, A., Nadjafi,

M., and Mahmudy-Gharaie, M.H., 2012. Geochemistry of Carboniferous sandstones (Sardar Formation), East-Central Iran: Implication for provenance and tectonic setting. *Acta Geologica Sinica* (English edition), 86(5): 1200–1210.

Ling Kunyue, Zhu Xiaoqing, Wang Zhonggang and Chen Wenyi, 2013. Discussion of the prospecting and searching strategy of laterite bauxite in Southern China. *Light Metals*, 414: 7–12 (in Chinese with English abstract).

Liu Ping, 2007. Characteristics of associate gallium distributed in the bauxite in Guizhou and its prospect for comprehensive utilization: Nine treatments of bauxite ores. *Guizhou Geology,* 24(2): 90–96 (in Chinese with English abstract).

Liu Wangchao, Yang Jiankuan and Xiao Bo, 2009. Review on treatment and utilization of bauxite residues in China. *International Journal of Mineral Processing*, 93: 220–231.

Liu Xuefei, Wang Qingfei, Deng Jun, Zhang Qizuan, Sun Silei and Meng Jianyin, 2010. Mineralogical and geochemical investigations of the Dajia Salento-type bauxite deposits, western Guangxi, China. *Journal of Geochemical Exploration*, 105: 137–152.

Liu Xunfeng, Wang Qingsheng, Chen Youneng and Qin Dianxie, 1990. *Bauxite Minerogenic Geological Characteristic and Minerogenic Law in Northern Guizhou, China*. Guiyang: Guizhou People's Publishing House, 131–136 (in Chinese).

MacLean W.H., Bonavia, F.F., and Sanna, G., 1997. Argillite debris converted to bauxite during karst weathering: evidence from immobile element geochemistry at the Olmedo deposit, Sardinia. *Mineralium Deposita*, 32: 607–616.

Maksimovic, Z., and Panto, G., 1991. Contribution to the geochemistry of the rare earth elements in the karst– bauxite deposits of Yugoslavia and Greece. *Geoderma*, 51: 93–109.

Mameli, P., Mongelli, G., Oggiano, G., and Dinelli, E., 2007. Geological, geochemical and mineralogical features of some bauxite deposits from Nurra (western Sardinia, Italy): insights on conditions of formation and parental affinity. *International Journal of Earth Sciences*, 96: 887–902 (Geologische Rundschau).

Masuda, A., Nakamura, N., and Tanaka, T., 1973. Fine structures isotope fractionation in the systems quartz-albite-anorthite. *Geochimica et Cosmochimica Acta*, 37: 239–248.

McDonough, W.F., Sun, S.-S., Ringwood, A.E., Jagoutz, E., and Hofmann, A.W., 1992. Potassium, rubidium, and cesium in the earth and moon and the evolution of the mantle of the earth. *Geochimica et Cosmochimica Acta*, 56: 1001–1012.

Mongelli, G., 1997. Ce-anomalies in the textural components of Upper Cretaceous karst bauxites from the Apulian carbonate platform (southern Italy). *Chemical Geology*, 140: 69–79.

Nesbitt, H.W., and Yong, G.M., 1982. Early Proterozoic climates and plate motions inferred from major element chemistry of lutites. *Nature*, 299: 715–717.

Öztürk, H., Hein, J.R., and Hanilci, N., 2002. Genesis of the Dogankuzu and Mortas bauxite deposits, Taurides, Turkey: Separation of Al, Fe, and Mn and implications for passive margin metallogeny. *Economic Geology*, 97: 1063–1077.

Qi Liang, Hu Jing and Gregoire, D.C., 2000. Determination of trace elements in granites by inductively coupled plasma mass spectrometry. *Talanta*, 51: 507–513.

Schroll, E., and Sauer, D., 1968. Beitrag zur geochemie von titan, chrom, nickel, cobalt, vanadium and molybdan in bauxitischen gestermenund problem der stofflichen herkunft des aluminiums. *Travaux du I'ICSOBA*, 5: 83–96.

Tang Yanjie, Jia Jianye and Liu Jianchao, 2001. Preliminary study on occurrence state of gallium in Dujiagou bauxite deposits and its controlling factors in the western areas of Henan Province. *Geology and Prospecting*, 37(6): 9–12 (in Chinese with English abstract).

Tang Yanjie, Jia Jianye and Liu Jianchao, 2002. Study on distribution laws of gallium in bauxite deposits in the western area of Henan Province. *Journal of Mineralogy and Petrology*, 22: 15–20 (in Chinese with English abstract).

Taylor, S.R., and McLennan, S.M., 1985. *The Continental Crust: Its Composition and Evolution*. Oxford: Blackwell, 312.

USGS, 2009. *Mineral Commodity Summaries: Bauxite and Alumina*. Washington: United States Government Printing Office, 1–8.

Valeton, I., 1972. *Bauxite, Development in Soil Science V.1*. London: Elsevier Publishing Company, 1–142.

Wang Junda and Li Huamei, 1998. Carboniferous paleo–latitude and bauxite deposits of central Guizhou Province. *Geochimica*, 27(6): 575–578 (in Chinese with English abstract).

Wang Yinchuan, Li Zhaokun, Zhai Zifeng, Li Ruibao and Li Xin, 2011. Benxi Formation bauxite mineralization condition and rule in Shanxi Province. *Northwestern Geology*, 44(4): 82–88 (in Chinese with English abstract).

Wu Guohui, Liu Youping and Zhang Yingwen, 2006. Geological characters and aluminum ore resources potential in the Wuchuan-Zhengan-Daozhen area, Guizhou. *Geology and Prospecting*, 42(2): 39–43 (in Chinese with English abstract).

Yang Ruidong, Yuan Shiting,Wei Huairui, Chen Jiyan Cheng Mali, 2011. Sediment geochemical character of Carboniferous "Qingzhen-type Fe deposit" in central Guizhou area. *geological review*, 57(1): 24–35 (in Chinese with English abstract).

Ye Lin, Cheng Zengtao and Pan Ziping, 2007. The REE geochemical characteristics of the Xiaoshanba bauxite deposit, Guizhou. *Bulletin of Mineralogy, Petrology and Geochemistry*, 26(3): 228–233 (in Chinese with English abstract).

Zarasvandi, A., Charchai, A., Carranza, E.J.M., and Alizadeh, B., 2008. Karst bauxite deposits in the Zagros mountain belt, Iran. *Ore Geology Reviews*, 34: 521–532.

Zhang Zhengwei, Li Yujiao, Zhou Lingjie, Wu Chengquan and Chaofei Zheng, 2013. The "coal-bauxite-iron" structure in the ore-bearing rock series as a prospecting indicator for southeastern Guizhou bauxite mines. *Ore Geology Reviews*, 53: 145–158.